
Advanced Composite Materials
Publication details, including instructions for authors and subscription information:
http://www.tandfonline.com/loi/tacm20

# Proposal of suppression of delamination for the foam core sandwich panel joint with filler

Y. Hirose , M. Nishitani , S. Ochi , K. Fukumoto , T. Kawasaki & M. Hojo

Version of record first published: 02 Apr 2012.

To cite this article: Y. Hirose , M. Nishitani , S. Ochi , K. Fukumoto , T. Kawasaki & M. Hojo (2006): Proposal of suppression of delamination for the foam core sandwich panel joint with filler, Advanced Composite Materials, 15:3, 319-339

To link to this article: http://dx.doi.org/10.1163/156855106778392061

*Adv. Composite Mater.*, Vol. 15, No. 3, pp. 319–339 (2006)

Also available online - www.brill.nl/acm



# Proposal of suppression of delamination for the foam core sandwich panel joint with filler *

Y. HIROSE [1,†], M. NISHITANI [1], S. OCHI [1], K. FUKUMOTO [1], T. KAWASAKI [1] and M. HOJO [2]

[1] *Kawasaki Heavy Industries, Ltd., 1.Kawasaki-cho, Kakamigahara City, Gifu-Pref. 504-8710, Japan*
[2] *Department of Mechanical Engineering and Science, Kyoto University, Sakyo-ku, Kyoto City, Kyoto Pref. 606-8501, Japan*

Received 30 May 2005; accepted 25 August 2005

**Abstract**—The failure mechanism of a foam core sandwich panel joint specimen was evaluated as future possible airplane fuselage structure. Specimens were manufactured from UT500/#135, graphite/epoxy fabric prepreg, and PEI (polyether imide) foam core and subjected to static tension in servo hydraulic loading frame. Delamination length, onset load and point were identified through the test. The energy release rate at the delamination end was calculated with the crack closure method in the fracture mechanics approach and the results were compared with the interlaminar fracture toughness value of UT500/#135 for ENF (End Notch Flexure) test. The calculated value of $G_{II}$ was much higher than the experimented fracture toughness values. The modified calculation with resin impregnation at the tapered core edge (filler) much reduced this difference. This fact also indicated that the resin filler improved the strength of foam core sandwich panel join.

*Keywords*: Sandwich structure; joint design; resin filler; delamination suppression.

## 1. INTRODUCTION

The co-cured design concept is essential to reduce structural weight and part count in the application of graphite/epoxy material to aircraft structures [1]. Five-year research activities were conducted to apply co-cured foam core sandwich panels to airplane nose structures. This study indicated that the replacement of the conventional built-up skin panel with the co-cured foam core sandwich panel led to considerable weight and part count reduction [2]. Fundamental researches of the foam core sandwich have already been conducted by various groups [3, 4].

*Edited by the JSCM.

†To whom correspondence should be addressed. E-mail: hirose_yasuo@khi.co.jp

The foam sandwich panel is already applied to maritime products [4]. As for the airplane application, Airbus Industries are conducting the research activities of foam core sandwich structure for fuselage skin panels [5]. In this application, a panel join is an inevitable structural element in the integral structure. It was also recognized that the joint configuration played an important role for the structural integrity because the joint is a structure element to transfer a load and a possible element for a fracture onset. Failure mechanism of the joint configuration should be investigated to assure the structural integrity when foam core sandwich panels are applied to aircraft primary structures. However, only a few researches have been carried out on the foam core sandwich panel joint in spite of its important role in the structural integrity. Though Bruman proposed a butt joint of the foam core itself, [2] this is not efficient from the structural point of view.

In the present study, the failure mechanism of miter-type joints, which have the butt splice at the solid laminate portion and also have the tapered core, was investigated from both experimental and analytical viewpoints. The effect of the resin impregnation at the tapered core edge on the onset of the delamination was studied with fracture mechanics approach.



## 2. EXPERIMENTAL AND ANALYTICAL METHOD

### *2.1. Experimental method*

*2.1.1. Joint test specimen.* A joint test specimen was employed to simulate the joint configuration of the aircraft nose structure made of foam core sandwich panels. The specimen is shown in Fig. 1. Joint specimens were manufactured from three different materials: Toho Tenax UT500/#135, graphite/epoxy twill weave fabric prepreg, PEI (polyether imide) foam core, and a 180°C cure class resin film (Syncore) with thickness of 0.254 mm. PEI foam core was ramped down to the solid laminate portion. Resin films were inserted between the skin graphite/epoxy laminates and the foam core. These resin plies were extended by 5 mm to the graphite/epoxy laminate from the tapered core edge as indicated in the enlarged part of Fig. 1. Each panel was co-cured in an autoclave. A butt-type joint concept was adopted (see Fig. 1). The two joint parts were mechanically fastened at the graphite/epoxy solid laminate portion with an aluminum splice plate and fasteners. The thickness of the aluminum plate was 8 mm. This plate was installed by the two rows of bolts without adhesive. The diameter of the bolts was 7.92 mm and the bolt space was 32 mm. This aluminum plate was simulated with bar element (CBAR) with comparable rigidity in the FEM analyses.

The thickness of the sandwich panel portion was 47 mm. The ply orientations of the graphite/epoxy skin panel were $\{[(+45, -45)/(0, 90)]_4\}_s$ with nominal thickness of 6.24 mm, and $\{[(+45, -45)/(0, 90)]_4\}_s/\{[(+45, -45)/(0, 90)]_4\}_s$ with nominal thickness of 12.48 mm for the skin plies over the core and solid laminate portion excluding resin film thickness, respectively. The resin content only adjacent to the

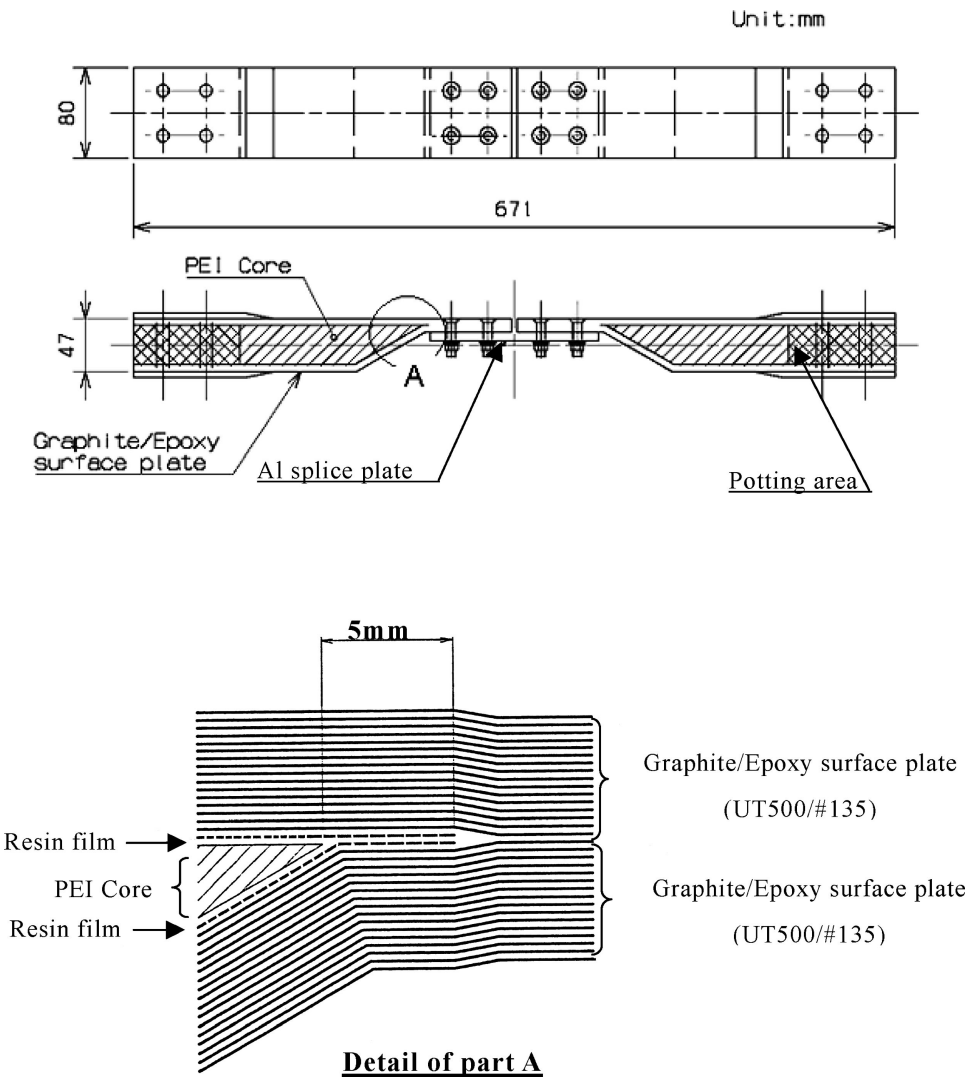


**Figure 1.** Joint test specimen.

foam core was increased from 35% to 45% to enhance the adhesion between core and prepreg for minimum thickness portions of sandwich panels. The mechanical properties of the material are summarized in Table 1.

A static test of the joint structure was conducted at room temperature under dry conditions. The servo hydraulic fatigue-testing machine with loading capacity of 50 kN was used for static tests at the crosshead speed of 1.27 mm/min. Figure 2 shows the loading apparatus together with the specimen and Fig. 3 shows the test set-up.

Four strain gages were bonded on the skin surface as indicated in Fig. 4.

**Table 1.**
Typical mechanical properties of the material

| | $E_1$ | $E_2$ | $G_{12}$ | $\nu_{12}$ | $G_{1Z}$ | $G_{2Z}$ | Remarks |
|---|---|---|---|---|---|---|---|
| PEI foam core | 0.0275 | 0.0275 | 0.0110 | 0.250 | — | — | |
| Resin film | 2.41 | 2.41 | 1.03 | 0.167 | — | — | |
| CFRP (0,90) | 54.9 | 8.61 | 3.77 | 0.331 | 3.53 | 3.77 | RC = 45% |
| CFRP (+45,−45) | 12.6 | 8.61 | 3.31 | 0.331 | 26.1 | 3.31 | RC = 45% |
| CFRP (0,90) | 66.3 | 8.61 | 3.77 | 0.331 | 4.24 | 3.77 | RC = 35% |
| CFRP (+45,−45) | 15.1 | 8.61 | 3.31 | 0.331 | 31.6 | 3.31 | RC = 35% |

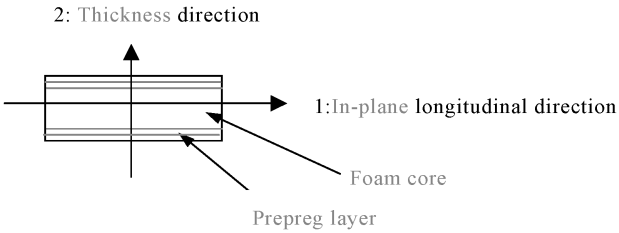


$E_1$: Stiffness in the in-plane longitudinal direction (GPa); $E_2$: Stiffness in the thickness direction (GPa); $G_{12}$: Shear stiffness in the 1-2 plane (GPa); $\nu_{12}$: Poisson's ratio; $G_{1Z}$: Shear stiffness in the 1-Z plane (GPa); $G_{2Z}$: Shear stiffness in the 2-Z plane (GPa); ($Z$-axis is perpendicular to the 1-2 plane); RC: Resin content by weight percent.

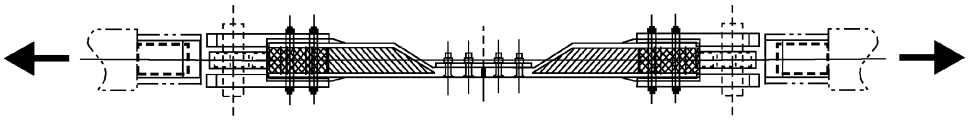

**Figure 2.** Loading apparatus of the joint specimen.

*2.1.2. Interlaminar fracture toughness test for UT500/#135.* Three-point ENF (end notch flexure) tests were conducted to obtain the mode II interlaminar fracture toughness values, $G_{\mathrm{IIC}}$. Five specimens were fabricated with 20 plies of (0,90) fabric and tested at room temperature under dry conditions. Tests were carried out based on JIS K 7086 [6–8] except for the crosshead speed of 2.54 mm/min. The cushion film between upper and lower side of the crack surface was also not introduced.

The following equation derived from the elastic beam theory was used as a crude estimation to calculate the $G_{\mathrm{IIC}}$ value [9].

$$G_{\mathrm{IIC}} = 9a^2P^2C/2W\left(2L^3 + 3a^3\right),$$

where $G_{\mathrm{IIC}}$ is the Mode II interlaminar fracture toughness ($J/\mathrm{m}^2$), $a$ is the crack length (m), $P$ is the critical load (N), $C$ is the compliance (m/N), $W$ is the specimen width (m), and $L$ is the half-length of the loading span (m).

The initial values of the fracture toughness, $G_{\mathrm{IIC}}$, were determined from the point of the deviation from the linearity in the initial load–displacement curve.

**Figure 3.** Test set-up.

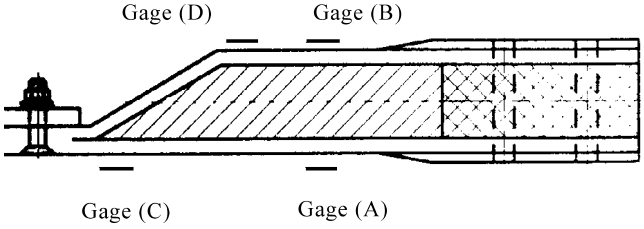


**Figure 4.** Strain gage locations.

## *2.2. Analytical method*

*2.2.1. FEM model for the tested specimen.* A two-dimensional finite element method (FEM) analysis for the joint configuration was conducted using commercial FEM code, NASTRAN.

The Model 1 is shown in Fig. 5. This model was prepared to simulate the global behavior of the joint specimen. In this model, each individual ply of a graphite/epoxy skin plies over the core and a resin film were modeled by a four-node quadratic plate element (CQUAD4) using the mechanical properties shown in Table 1. The PEI core was also modeled as isotropic material. The difference of resin weight fraction for applicable plies was taken into consideration in the analysis. The test fixture was also modeled with rigid bar elements and spring elements to simulate end fixtures and universal joints. The analysis was conducted under the

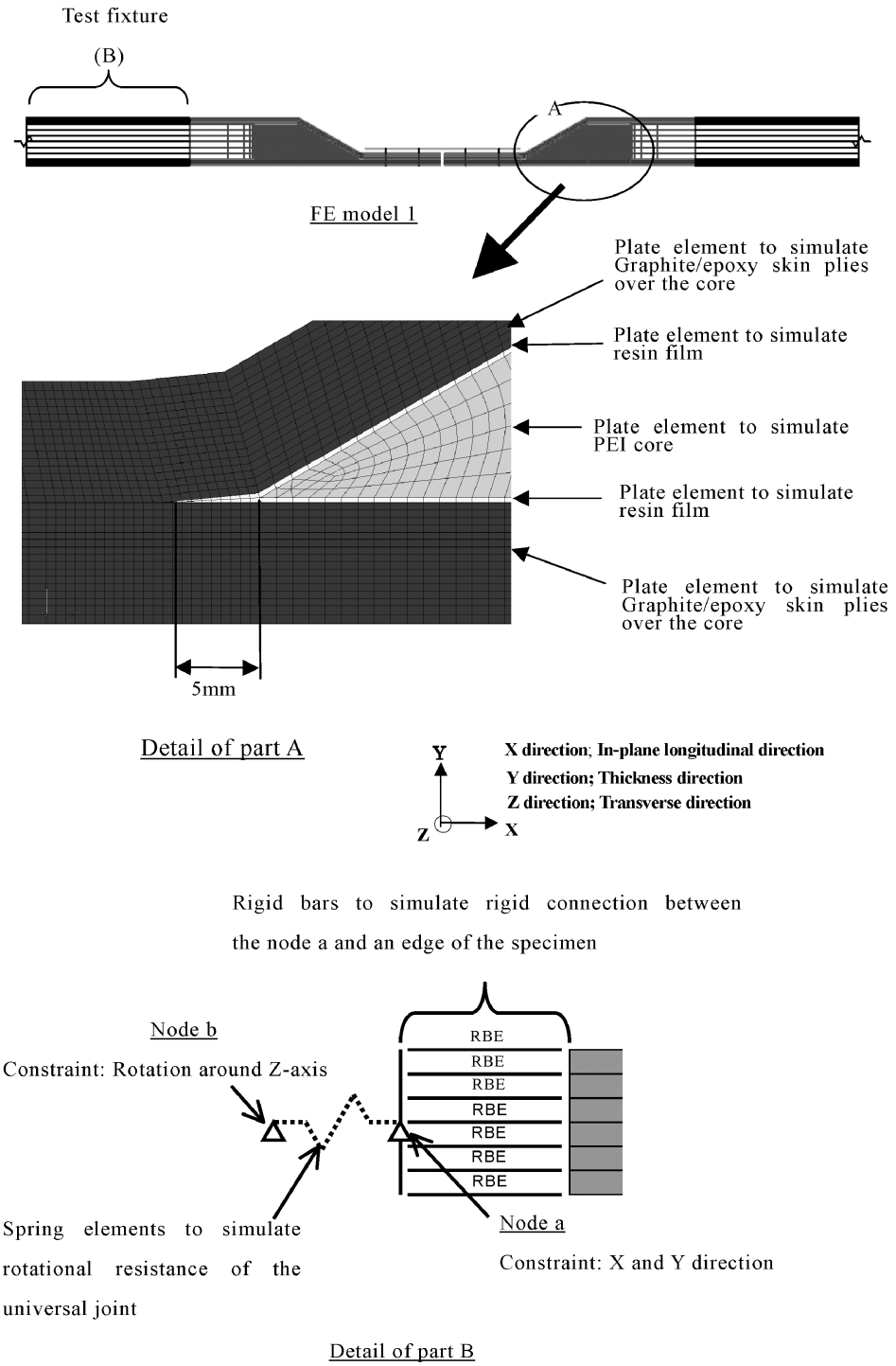


**Figure 5.** FE Model 1 of the joint.

large deformation analysis with tension loading of 39.2 kN to meet the experimental results. The verification of this FE analyses was done by the comparison between experimental and analytical strain measurements shown in Fig. 4.

*2.2.2. FEM model to calculate energy release rate.* Large deformation FEM analyses of the joint were conducted to calculate the exact energy release rate at the delamination end. Two types of FE models, such as Model 2 and Model 3, were used.

The Model 2 shown in Fig. 6 was prepared to modify the Model 1 by introducing delamination. The initial delamination was divided into the following three parts: (a) the delamination with the length of 2 mm into the solid laminate portion from the end of the resin film, (b) the delamination with 5 mm length between resin films from the tapered core edge, and (c) the delamination between resin film and foam core. The enlarged FE model at the tapered core edge is shown in Fig. 6 with this delamination.

The Model 3 shown in Fig. 7 was prepared to modify the Model 2 in order to simulate the resin impregnation region at the tapered core edge. This region was observed through the detailed investigation for the cut specimen (see Fig. 15). Here, the mechanical properties of five elements at the tapered core edge were replaced from PEI ones to resin ones in order to simulate the resin impregnation region (see the enlarged part in Fig. 7).

*2.2.3. FE model to estimate the effect of filler.* The FE Model 4 was prepared in order to estimate, through parametric studies, the effect of inserting artificial filler with different properties on the energy release rate at an expected onset point of delamination with the length of 0.33 mm. As for the Model 4, the mechanical properties of ten elements at the tapered core edge were parametrically changed from foam core properties to various ones including those of the resin and CFRP UD material in order to estimate the effect of the filler properties. The Model 4 is shown in Fig. 8.

A Model 5 was also prepared to investigate the effect of the filler size on the energy release rate at an expected onset point of the delamination with the same length as that of Model 4. The size of the filler was changed parametrically for comparison. The Model 5 is shown in Fig. 9. A parameter X shown in Fig. 9 was defined as the length from the tapered core edge to the end of the filler. The range of X was decided from 0 to 58.9 mm corresponding to the entire range of the tapered area.

## 3. RESULTS AND DISCUSSION

### *3.1. Experimental results*

*3.1.1. Joint test results.* Figure 10a shows the relation between the load and strain measured by the gages from (A) to (D), as explained for Fig. 4. Delamination

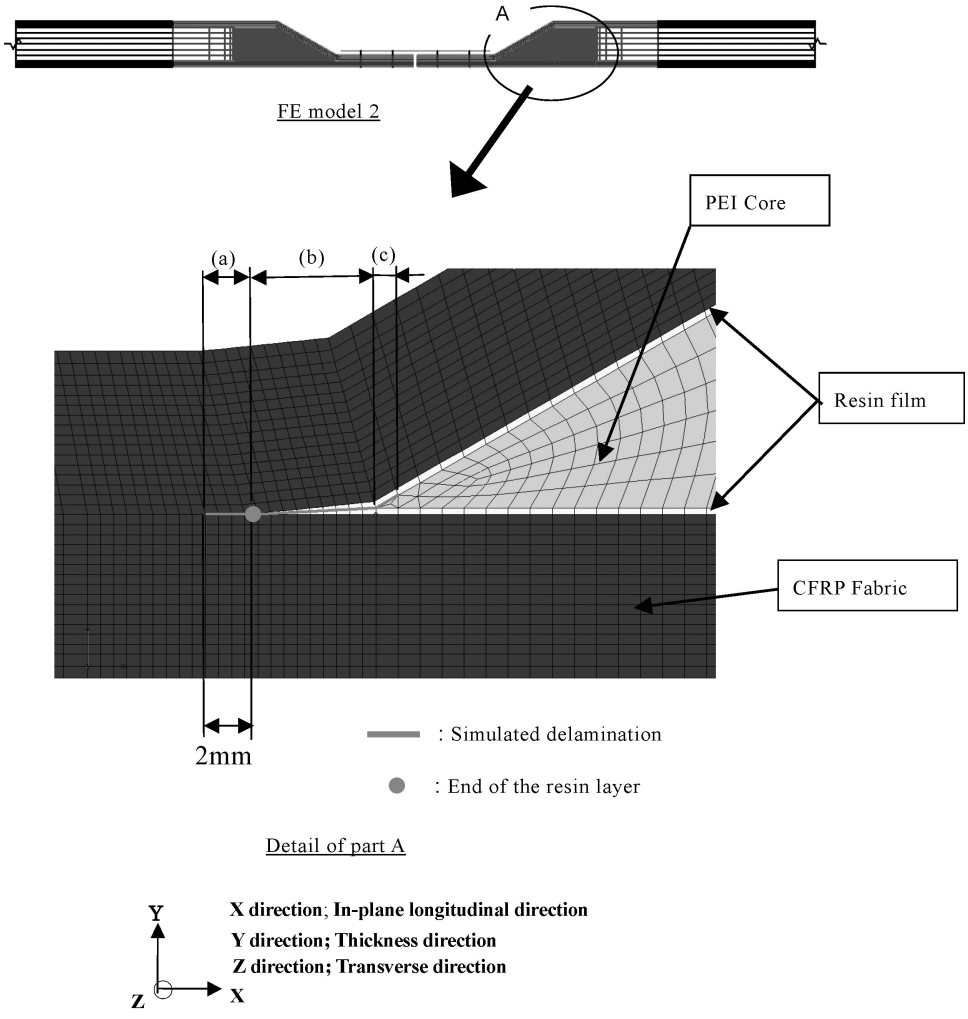


**Figure 6.** FE Model 2 of the joint.

initiated from the end of the resin film at the tapered core edge into the solid laminate as shown in Fig. 10b. The total delamination length from the tapered core edge was 7 mm at an initial failure load of 39.2 kN. The joint structure integrity was hampered by this delamination. Thus, this delamination was regarded as a structural failure from the design point of view. The rapid change of the load–strain diagram for the strain gage C clearly indicated the onset of the delamination. However, no changes were observed for the measurement of other gages. Since the length of the delamination was limited to 7 mm at the tapered core edge, the global deformation behavior remained unchanged. The compressive strain was observed for the gages (c) and (d) owing to the local bending deformation.

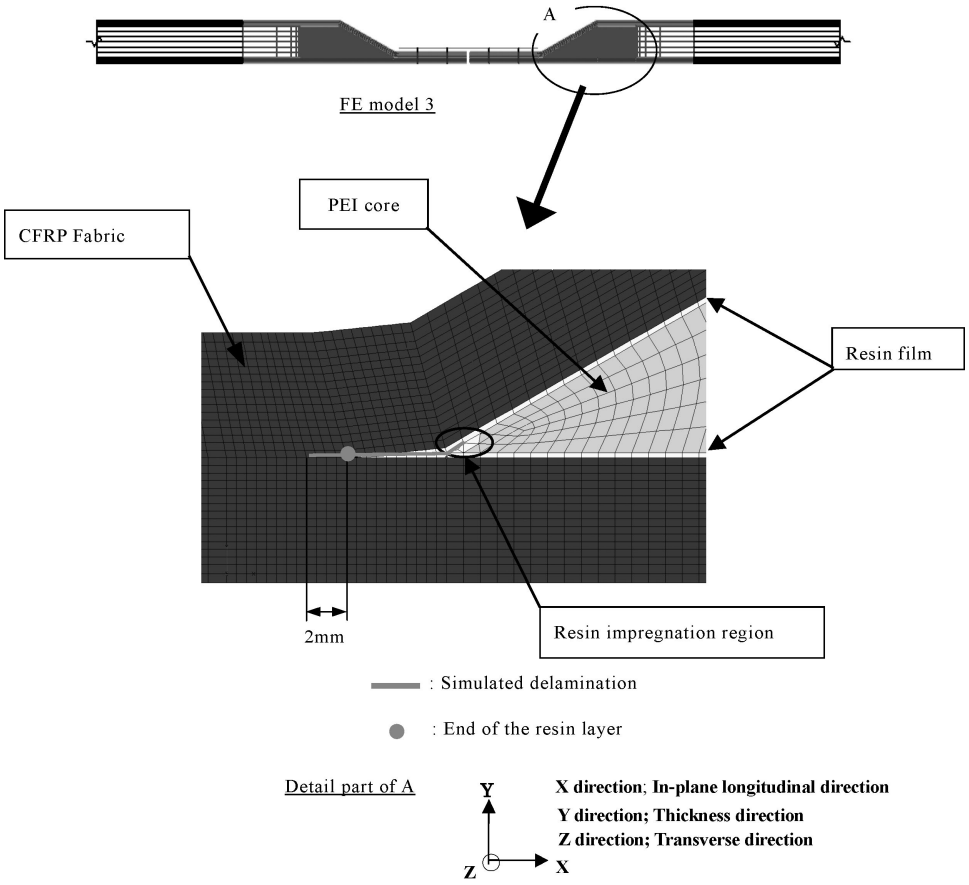


**Figure 7.** FE Model 3 of the joint.

The final failure occurred at 107.8 kN as a bearing failure of the fastener. The macroscopic failure morphology and detail failure mode are shown in Fig. 11. The delamination propagated to two directions as indicated by white thin dotted arrows from the tapered core edge following the initial onset of delamination as shown by the white thick solid allows in Fig. 11b.

*3.1.2. Interlaminar fracture toughness test results for UT500/#135.* The typical relation between load and displacement for three-point ENF tests is shown in Fig. 12. The average $G_{\mathrm{IIC}}$ of the UT500/#135 for the NL point was 1.53 kJ/m$^2$ and the standard deviation, 0.06 kJ/m$^2$, were obtained through the tests.

### *3.2. Analytical results*

*3.2.1. FEM analysis for joint test specimen.* The deformation diagram derived from FEM analyses is shown in Fig. 13. This diagram shows the specimen is

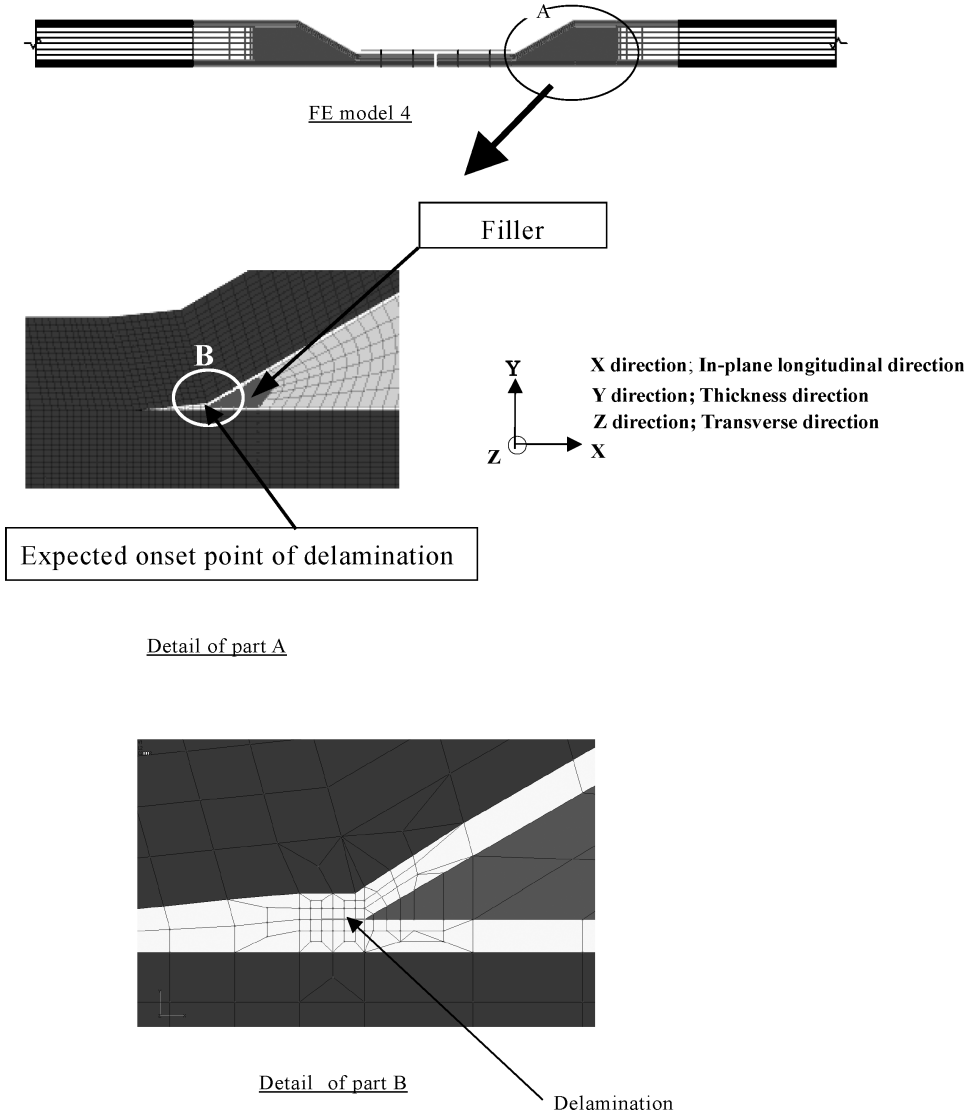


**Figure 8.** FE Model 4 of the joint.

deformed in a convex shape. This unbalanced loading between upper and lower skins brings shear stress at the tapered core edge. This analytical result supports the onset point of the delamination in the experimental results. Similar mechanism to originate delamination is reported for a tapered laminate with a ply-drop [10].

The strain values calculated with FEM analysis at the gage locations were compared with the test results in Fig. 14. This comparison indicates the small discrepancy between analytical results and experimental ones because the test specimen together with loading fixture was modeled using two-dimensional elements. The loading path in the FE model was supposed to be different from the actual one in

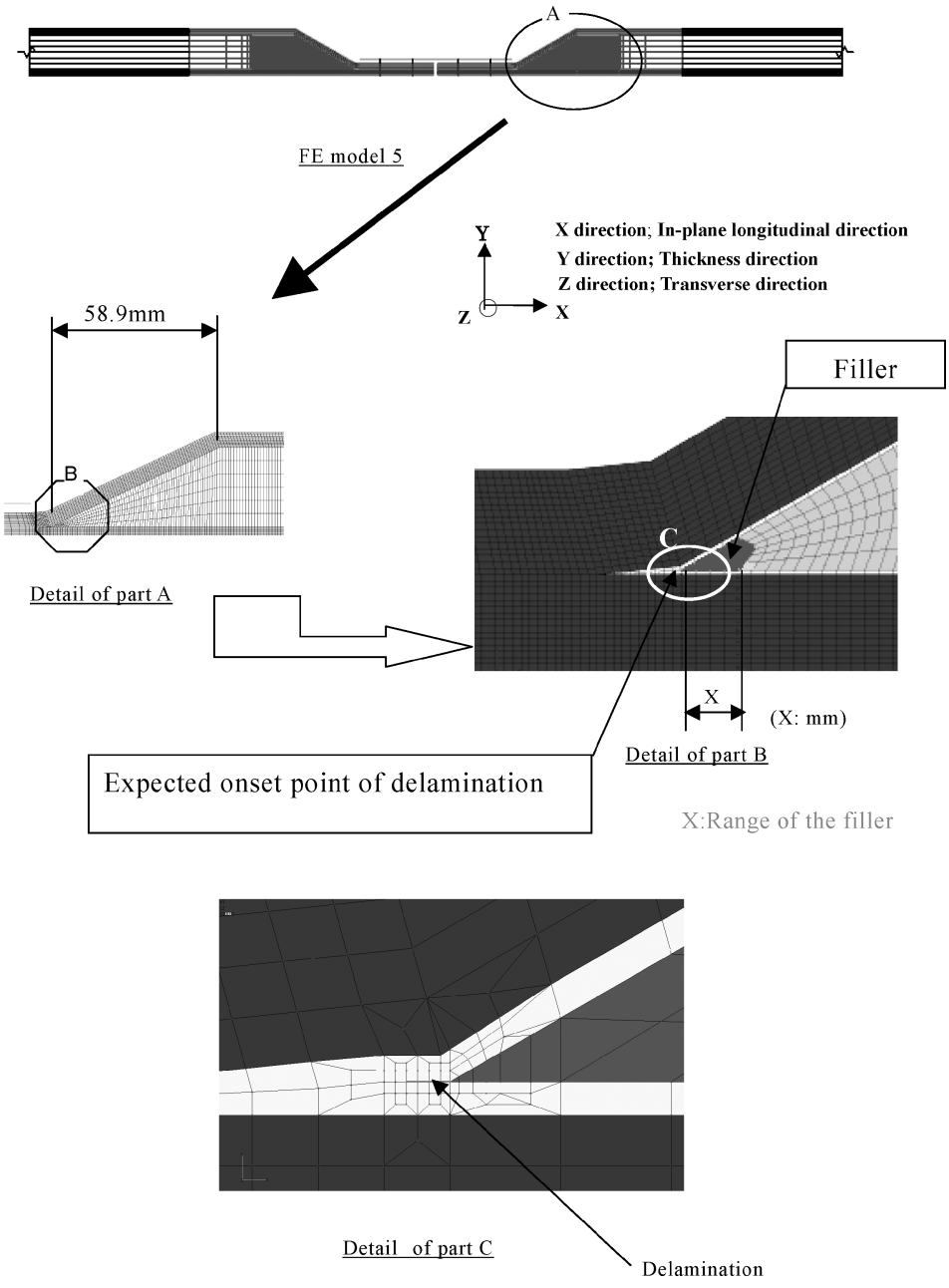


**Figure 9.** FE Model 5 of the joint.

the test specimen in the two-dimensional modeling since three-dimensional parts such as fasteners and loading fixtures could not be simulated accurately with a two-dimensional model.

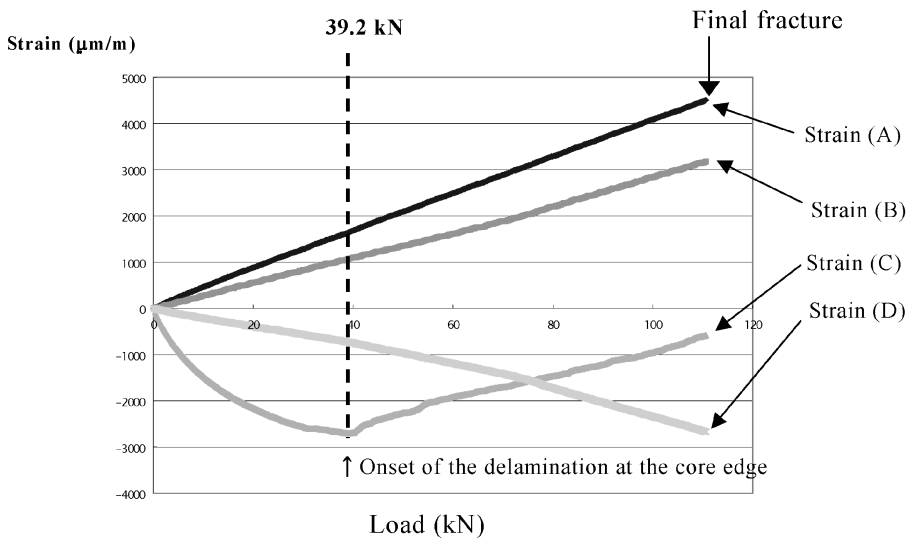


(a) Load – Strain Diagram.

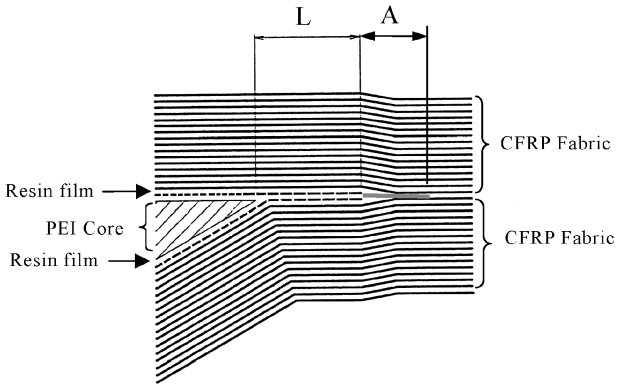


**A: Observed delamination length of 2mm between CFRP fabric layer**

**L: Observed delamination length into solid laminate portion of 5mm between resin film**

(b) Onset of delamination

**Figure 10.** Load–strain diagram and situation of delamination.

*3.2.2. Energy release rate at the delamination end.* Energy release rates of $G_{\mathrm{I}}$ and $G_{\mathrm{II}}$ at the delamination end were calculated using the crack closure method [11] for the Model 2 shown in Fig. 6. The results are indicated in Table 2. This table and the deformation diagram of the specimen shown in Fig. 13 indicate that the crack is under almost pure Mode II condition and its energy release rate is 2.12 kJ/m$^2$ at the tensile fracture load of 39.2 kN. This energy release rate is much higher than

(a) Macroscopic failure morphology

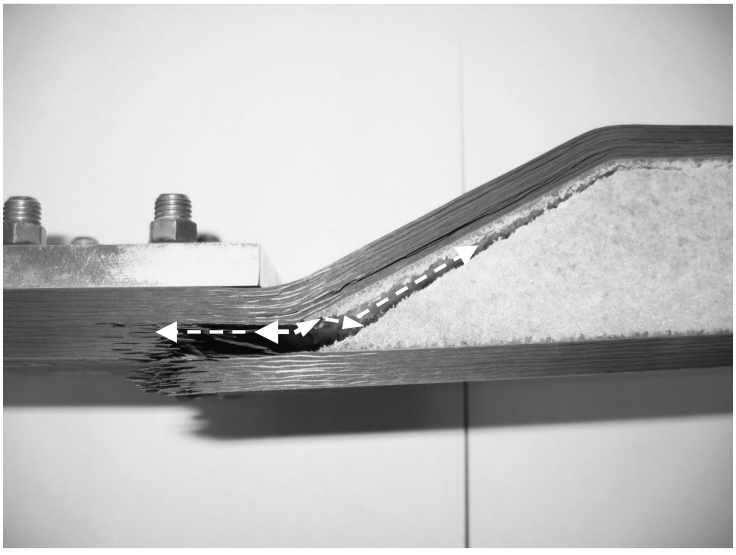

(b) Detail failure mode

**Figure 11.** Final failure.

the interlaminar fracture toughness value of 1.53 kJ/m$^2$ for UT500/#135 using ENF tests.

The cross-section of the test specimen was observed in order to investigate the reason for this difference. Through this observation, resin impregnation to the core material was found at the tapered core edge. The cross-section of the specimen is

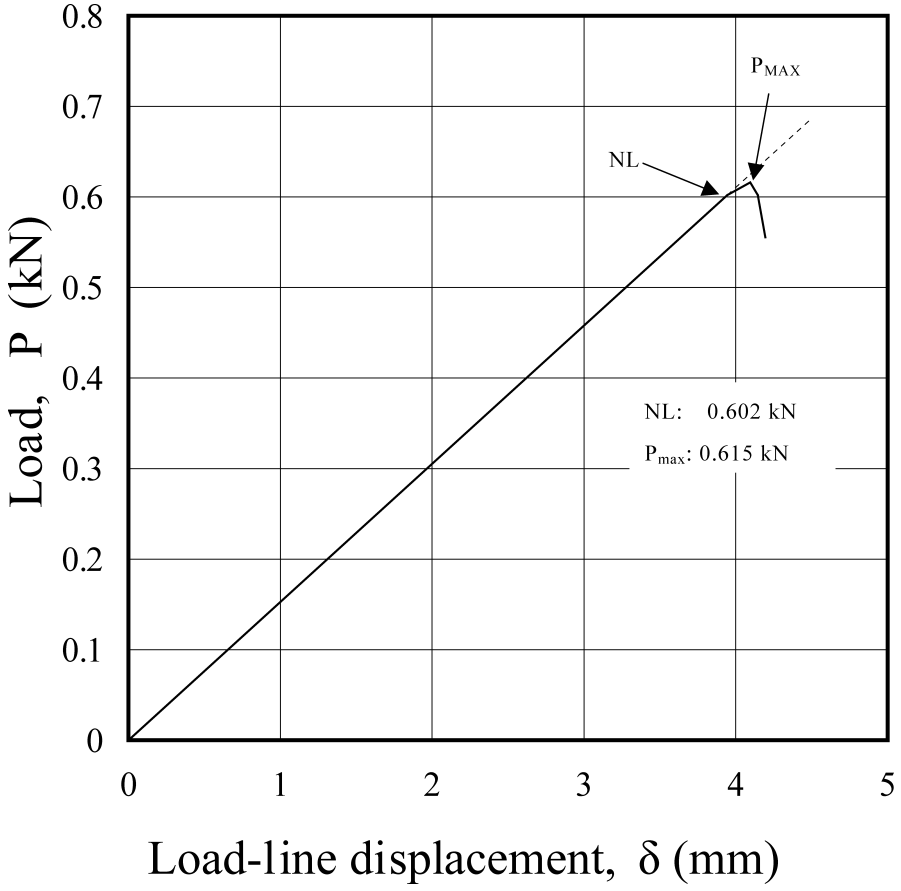


**Figure 12.** Relation between load and displacement for 3-point ENF tests.

**Table 2.**
Calculated energy release rate

| Energy release rate | Model 2 | Model 3 |
|---|---|---|
| $G_{\mathrm{I}}$ (kJ/m$^2$) | 0.06 | 0.06 |
| $G_{\mathrm{II}}$ (kJ/m$^2$) | 2.12 | 1.53 |

shown in Fig. 15. This resin impregnation probably comes from the squeezed resin from UT500/#135 prepreg. It is supposed that resin flow merged into the core cells during the autoclave cure process. Then, FEM analysis for the Model 3 shown in Fig. 7, which simulated this resin impregnation, was conducted, and the value of $G_{\mathrm{II}}$ obtained was 1.53 kJ/m$^2$, as shown in Table 2. This value is very close to the interlaminar fracture toughness value of 1.53 kJ/m$^2$ for UT500/#135.

In order to discuss the effect of the resin impregnation on the energy release rate, the $\tau_{XY}$ distribution for the Model 2 and the Model 3 are shown in Fig. 16.

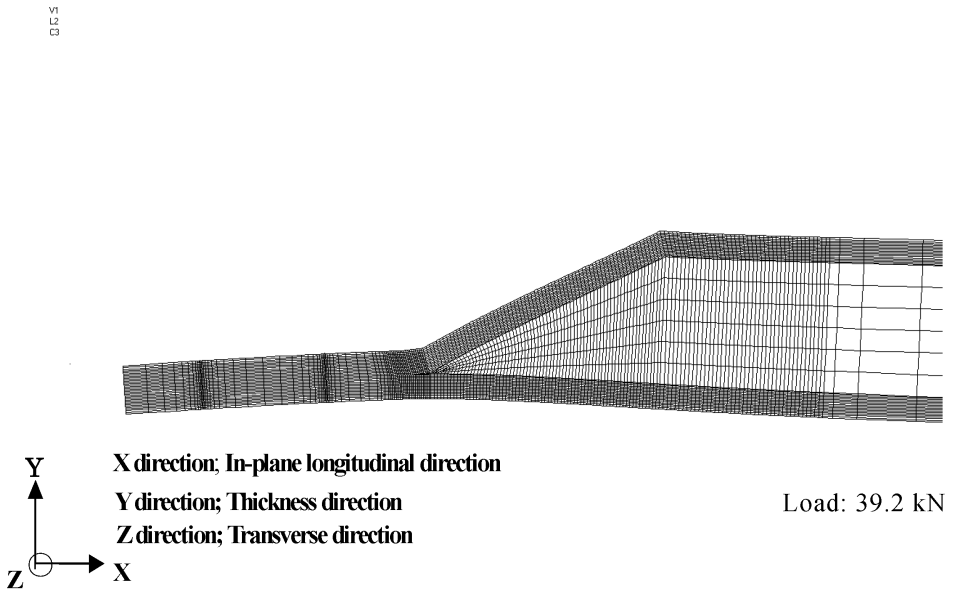


**Figure 13.** Deformation diagram derived from FEM analysis.

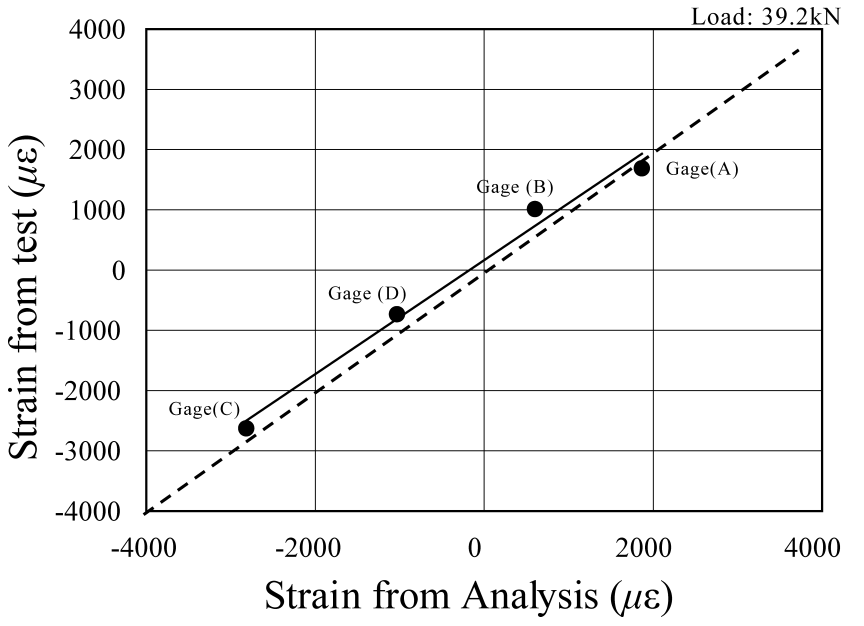


**Figure 14.** Comparison of the strain distribution.

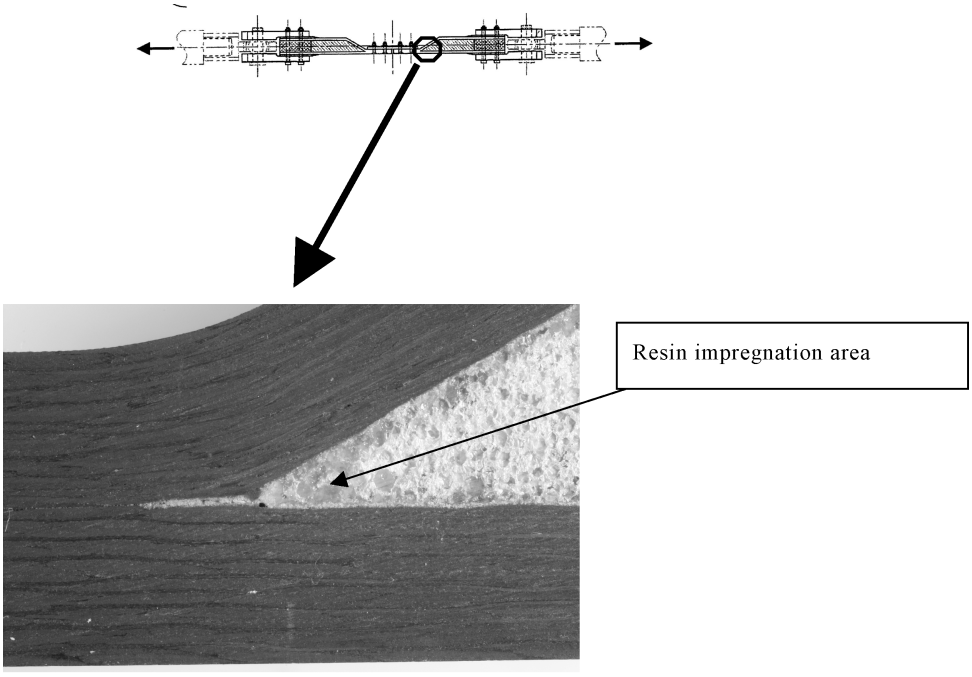


**Figure 15.** Resin impregnation region of the specimen.

Comparison of these two $\tau_{XY}$ distributions indicates that the resin impregnation region sustains some amount of load and decreases the stress concentration at the delamination end. This is why the $G_{\mathrm{II}}$ of 2.21 kJ/m$^2$ was reduced to 1.53 kJ/m$^2$ by the resin impregnation.

*3.2.3. Effect of the filler on the stress distribution.* The above results reveal that dissimilar material in the foam core, such as resin impregnation at the tapered core edge, suppresses the energy release rate of the delamination end and also onset of the delamination for a foam core sandwich panel joint. This result indicates that it is possible to improve the joint design of the foam core sandwich panel by the introduction of dissimilar material, such as the resin filler at the tapered core edge. In order to confirm this idea, FEM analyses using the Models 4 and 5 were conducted for unit load and energy release rate at the expected onset point of delamination with the length of 0.33 mm were calculated.

The fillers were inserted at the tapered core edge with various mechanical properties in the Model 4. The effect of the mechanical properties of the filler on the energy release rate at the expected point of the delamination onset is shown in Fig. 17. The energy release rates for each case were normalized with respect to the energy release rate without filler case. The energy release rate at the expected point of delamination decreases as the shear modulus of the filler increases. This diagram

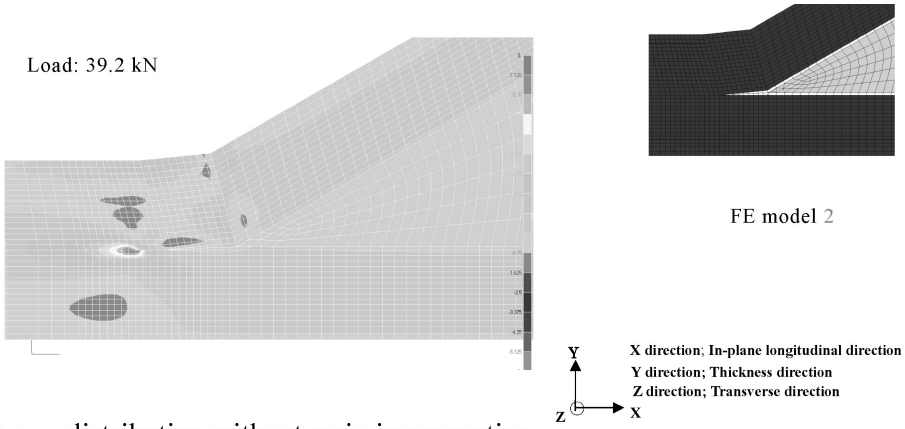


(a). $\tau_{XY}$ distribution without resin impregnation

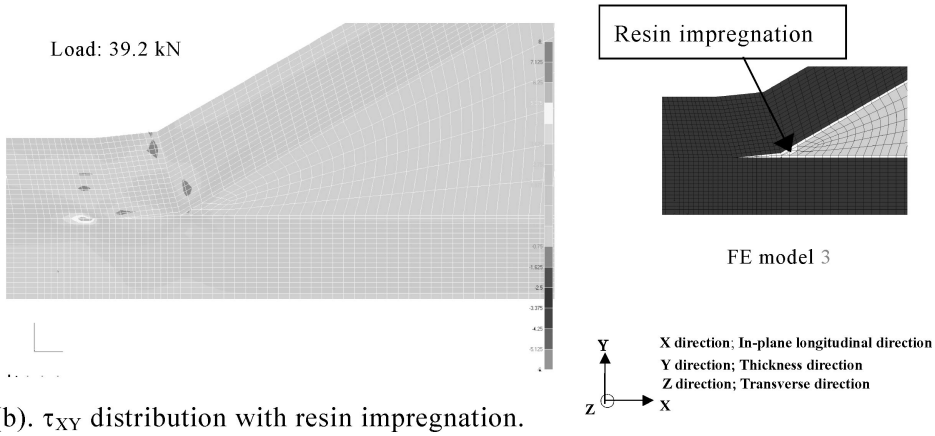


(b). $\tau_{XY}$ distribution with resin impregnation.

**Figure 16.** Comparison of $\tau_{XY}$ distribution with and without resin filler.

shows that the filler with the mechanical properties of resin is enough to reduce the energy release rate. Only a small difference of the normalized energy release rate was observed between filler properties of resin and CFRP. The $\tau_{XY}$ distribution for the resin filler is shown in Fig. 18 as a typical case. The similar effect to the resin impregnation case shown in Fig. 16 was observed in this figure.

The effect of the filler area on the energy release rate at the expected onset point of the delamination is shown in Fig. 19. This diagram indicates that a relatively small area of the filler, such as 5 mm from the tapered core edge, has a significant effect on the energy release rate reduction.

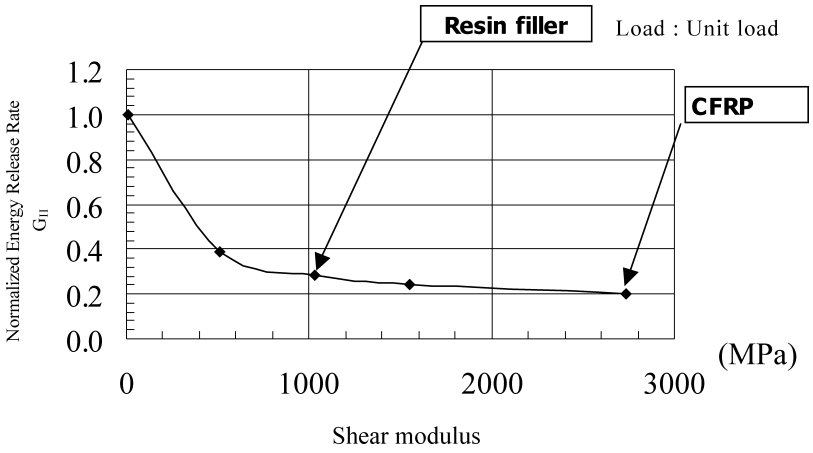


**Figure 17.** The effect of the filler area.

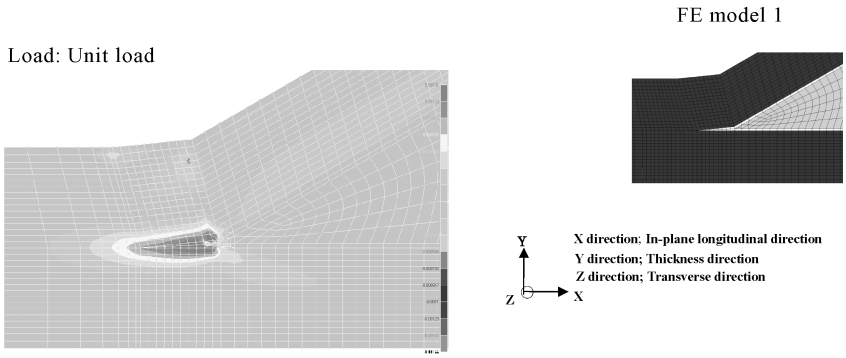


(a) $\tau_{XY}$ distribution without resin filler (Model 1).

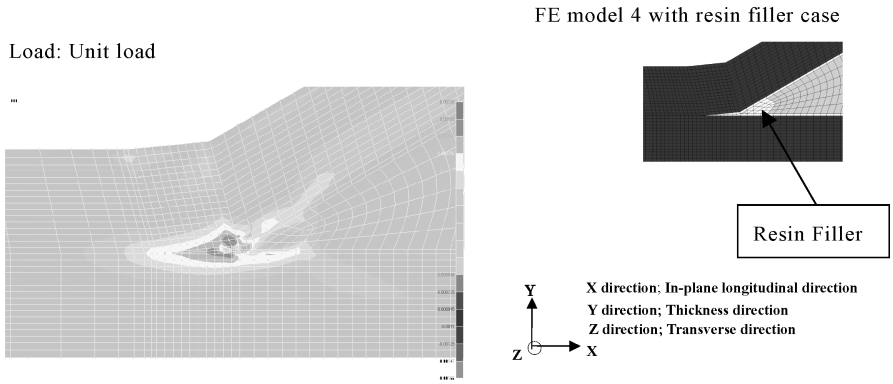


(b) $\tau_{XY}$ distribution with resin filler (Model 4 with resin filler case)

**Figure 18.** $\tau_{XY}$ distribution with and without resin filler.

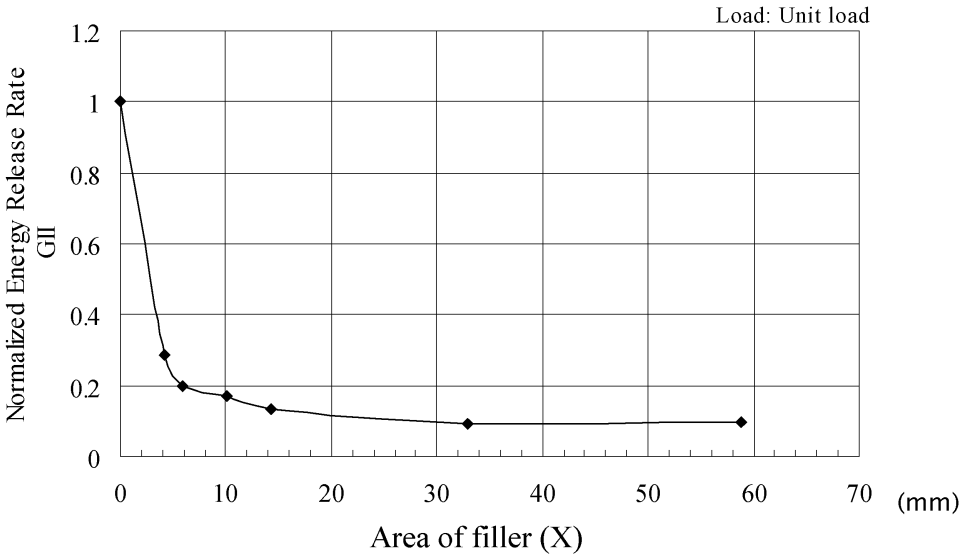


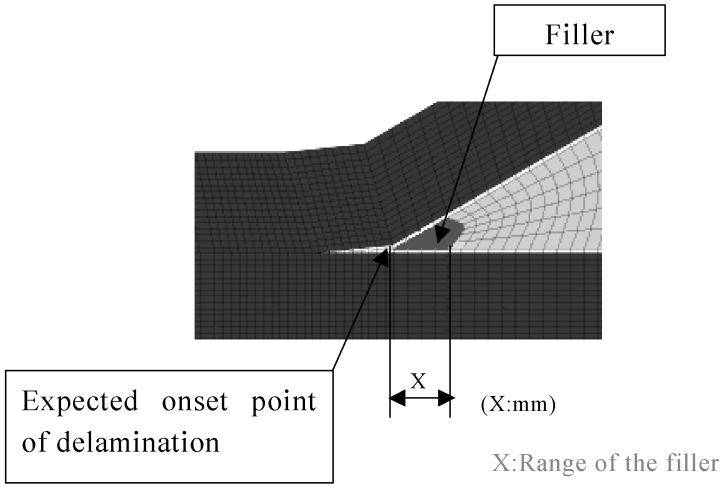


**Figure 19.** The effect of the filler area.

Figures 17 and 19 indicate that the introduction of a resin filler in the limited area of the tapered core edge is a simple method to improve the join design.

The energy release rate is largely dependent on the mesh pattern and element in the FEM analysis. But this comparison was conducted with the same mesh pattern and the same element. The relative comparison of the energy release rate is reasonable for the present study.

## 4. CONCLUDING REMARKS

The effect of resin filler at the tapered core edge was shown both experimentally and analytically to suppress delamination onset. The results are summarized as follows.

The calculated energy release rate at delamination end using the crack closure method was compared with the interlaminar fracture toughness value of UT500/#135 for ENF test. The calculated value of the energy release rate, $G_{\mathrm{II}}$, at delamination onset load was much higher than the experimented fracture toughness values, $G_{\mathrm{IIC}}$.

The existence of resin impregnation at the tapered core edge much reduced the $G_{\mathrm{II}}$ values. The $G_{\mathrm{II}}$ values with this modified calculation agreed well with the $G_{\mathrm{IIC}}$ value.

A simple method to suppress the initiation of the delamination for a foam core sandwich panel joint was proposed with a resin filler insert based on the fracture mechanics approach.

*Acknowledgement*

The authors would like to acknowledge their appreciation for JADC (Japan Aircraft Development Corporation) in providing technical support for this program, especially to Dr. Kikukawa (now, Professor at the Kanazawa Institute of Technology) and Mr. Yahata (now at Churyo Engineering) and NEDO (New Energy and Industrial Technology Development Organization) for their financial support of this program.



## REFERENCES

1. Y. Hirose, T. Taki, Y. Mizusaki and T. Fujita, Low cost structural concept for composite trailing edge flap, *Adv. Composite Mater*. **12**, 281–300 (2004).
2. Y. Hirose, M. Nishitani, M. Imuta, H. Fukagawa and H. Kikukawa, Development of foam core sandwich panel structure for transport nose component, SME Technical Paper TP03PUB317 (2003).
3. M. Bruman, Fatigue crack initiation and propagation in sandwich structures, Report No. 98-29, Department of Aeronautics, Royal Institute of Technology, Stockholm, Sweden (1997).
4. A. Shipsha, Failure of sandwich structures with sub-interface damage, Report 2001-13, Department of Aeronautics, Royal Institute of Technology, Stockholm, Sweden (2001).
5. L. Herbeck, H. Wilmes and M. Kleineberg, Material and processing technology for CFRP fuselage, SAMPE USA (2004).
6. JIS K 7086 Testing methods for interlaminar fracture toughness of carbon fiber reinforced plastics.
7. M. Hojo, K. Kageyama and Y. Tanaka, Prestandardization study on mode I interlaminar fracture toughness test for CFRP in Japan, *Composites* **26**, 243 (1995).
8. Y. Tanaka, K. Kageyama and M. Hojo, Prestandardization study on mode II interlaminar fracture toughness test for CFRP In Japan, *Composites* **26**, 57 (1995).
9. A. J. Russell and K. N. Street, Moisture and temperature effects on the mixed-mode delamination fracture of unidirectional graphite/epoxy, in: *ASTM STP876*, W. S. Johnson (Ed.), pp. 349–370. American Society for Testing and Materials, Philadelphia (1985).

10. G. B. Murri, S. A. Salpekar and T. K. O'Brien, Fatigue delamination onset prediction in unidirectional tapered laminates, in: *Composite Materials: Fatigue and Fracture*, *ASTM STP1110*, Vol. 3, T. K. O'Brien (Ed.), pp. 312–339. American Society for Testing and Materials, Philadelphia (1991).
11. E. F. Rybicki and M. F. Kanninen, A finite element calculation of stress intensity factors by a modified crack closure integral, *Engng. Fract. Mech.* **9**, 931–938 (1977).